

Efficient Cosmological Parameter Estimation from Microwave Background Anisotropies

Arthur Kosowsky,^{*} Milos Milosavljevic,[†] and Raul Jimenez[‡]

*Department of Physics and Astronomy, Rutgers University,
136 Frelinghuysen Road, Piscataway, New Jersey 08854-8019*

(Dated: May, 2002)

We revisit the issue of cosmological parameter estimation in light of current and upcoming high-precision measurements of the cosmic microwave background power spectrum. Physical quantities which determine the power spectrum are reviewed, and their connection to familiar cosmological parameters is explicated. We present a set of physical parameters, analytic functions of the usual cosmological parameters, upon which the microwave background power spectrum depends linearly (or with some other simple dependence) over a wide range of parameter values. With such a set of parameters, microwave background power spectra can be estimated with high accuracy and negligible computational effort, vastly increasing the efficiency of cosmological parameter error determination. The techniques presented here allow calculation of microwave background power spectra 10^5 times faster than comparably accurate direct codes (after precomputing a handful of power spectra). We discuss various issues of parameter estimation, including parameter degeneracies, numerical precision, mapping between physical and cosmological parameters, and systematic errors, and illustrate these considerations with an idealized model of the MAP experiment.

PACS numbers: 98.70.V, 98.80.C

I. INTRODUCTION

By January 2003, microwave maps of the full sky at 0.2° resolution will be available to the world, the harvest of the remarkable MAP satellite currently taking data [1]. The angular power spectrum of the temperature fluctuations in these maps will be determined to high precision on angular scales from the resolution limit up to a dipole variation; this corresponds to about 800 statistically independent power spectrum measurements. Recent measurements have given a taste of the data to come, although covering much smaller patches of the sky and with potentially more serious systematic errors [2, 3, 4].

The main science driving these spectacular technical feats is the determination of basic cosmological parameters describing our Universe, and resulting insights into fundamental physics; see [5, 6] for recent reviews and [7] for a pedagogical introduction. The expected series of acoustic peaks in the microwave background power spectrum encode enough information to make possible the determination of numerous cosmological parameters *simultaneously* [8]. These parameters include the long-sought Hubble parameter H_0 , the large-scale geometry of the Universe Ω , the mean density of baryons in the Universe Ω_b , and the value of the mysterious but now widely accepted cosmological constant Λ , along with parameters describing the tiny primordial perturbations which grew into present structures, and the redshift at which the Uni-

verse reionized due to the formation of the first stars or other compact objects. While most of these parameters and other information will be determined to high precision, one near-exact degeneracy and other approximate degeneracies exist between these parameters [9, 10].

The exciting prospects of providing definitive answers to some of cosmology's oldest questions raise a potentially difficult technical issue, namely finding constraints on a large-dimensional parameter space. Given a set of data, what range of points in parameter space give models with an acceptably good fit to the data? The answer requires evaluating a likelihood function at many points in parameter space; in particular, finding confidence regions in multidimensional parameter space requires looking around in the space. This is a straightforward process, in principle. But a parameter space with as many as ten dimensions requires evaluating a lot of models: a grid with a crude 10 values per parameter contains ten billion models. A direct calculation of this many models is prohibitive, even with very fast computers. While some of the parameters are independent of the others (i.e. tensor modes), reducing the effective dimensionality, many of the parameters will be constrained quite tightly, requiring a finer sampling in that direction of parameter space. An additional problem with brute-force grid-based methods is a lack of flexibility: if additional parameters are required to correctly describe the Universe, vast amounts of recalculation must be done. Grid-based techniques have been used for analysis of cosmological parameters from microwave background (e.g., [11, 12]) but clearly this method is not fast or flexible enough to deal with upcoming data sets adequately.

A more sophisticated approach is to perform a search of parameter space in the region of interest. Relevant techniques are well known and have been applied to the

^{*}Also at School of Natural Sciences, Institute for Advanced Study, Einstein Drive, Princeton, New Jersey 08540 ; Electronic address: kosowsky@physics.rutgers.edu

[†]Electronic address: milos@physics.rutgers.edu

[‡]Electronic address: raulj@physics.rutgers.edu

microwave background [13, 14, 15]. Reliable estimates of the error region in cosmological parameter space can be obtained with random sets of around 10^5 models, reducing the computational burden by a factor of 1000 or more compared to the cruder grid search methods. On fast parallel computers it is possible to compute the power spectrum for a given model in a computation time on the order of a second [16], making Monte Carlo error determinations feasible. For improved efficiency, useful implementations do not recalculate the entire spectrum at each point in parameter space, but rather use approximate power spectra based on smaller numbers of calculated models [17].

Here we expand and refine this idea by presenting a set of parameters, functions of the usual cosmological parameters, which reflect the underlying physical effects determining the microwave background power spectrum and thus result in particularly simple and intuitive parameter dependences. Previous crude implementations of this idea applied to low-resolution measurements of the power spectrum [18]; the current and upcoming power spectrum measurements requires a far more refined implementation. Our set of parameters can be used to construct computationally trivial but highly accurate approximate power spectra, and large Monte Carlo computations can then be performed with great efficiency. Additional advantages of a physically-based parameter set are that the degeneracy structure of the parameter space can be seen much more clearly, and the Monte Carlo itself takes significantly fewer models to converge.

Earlier Fisher-matrix approximations of parameter errors are a rough implementation of this general idea: if the the power spectrum varies exactly linearly with each parameter in some parameter set, and the measurement errors are gaussian random distributed and uncorrelated, then the likelihood function as a function of the parameters can be computed *exactly* from the partial derivatives of the model with respect to the parameters [8, 19, 20]. Even if the linear parameter dependence does not hold throughout the parameter space, it will almost always be valid in some small enough region, being the lowest-order term in a Taylor expansion. If this region is at least as large as the resulting error region, then the Fisher matrix provides a self-consistent approximation for error determination. The difficulty is in finding a suitable parameter set. Our aim is not necessarily to find a set of parameters which all have a perfectly linear effect on the power spectrum. Rather, more generally, we desire a set of parameters for which the power spectrum can be approximated very accurately with a minimum of computational effort. Then we can dispense with approximations of the likelihood function, as in the Fisher matrix approach, and directly implement a Monte Carlo parameter space search with a minimum of computational effort. This technique allows simple incorporation of prior probabilities determined from other sources of data, and if fast enough allows detailed exploration of potential systematic biases in parameter values arising from numerous

experimental and analysis issues such as treatment of foregrounds, noise correlations, mapmaking techniques, and model accuracy.

We emphasize that with the accuracy of upcoming microwave background power spectrum measurements, the cosmological parameters will be determined precisely enough that their values will be significantly affected by systematic errors from assumptions made in the analysis pipeline and, potentially, numerical errors in evaluating theoretical power spectra. The measurements themselves may also be dominated by systematic errors. Extensive modelling of the impact of various systematic errors on cosmological parameter determination will be *essential* before any parameter determination can be considered reliable. This is the primary motivation for increasing the efficiency of parameter error analysis. We discuss this point in more detail in the last Section of the paper.

The following Section reviews physical processes affecting the cosmic microwave background and defines our physical parameter set. The key parameter, which sets the angular scale of the acoustic oscillations, has been discussed previously in similar contexts [10, 21, 22] but has not been explicitly used as a parameter. The other parameters describing the background cosmology can then be chosen to model other specific physical effects. Section III displays how the power spectrum varies as each parameter changes with the others held fixed. The mapping between our physical parameters and the conventional cosmological parameters immediately reveals the structure of degeneracies in the cosmological parameter space. Simple approximations for the effect of each physical parameter are shown to be highly accurate for all but the largest scales in the power spectrum. We then determine the error region in parameter space for an idealized model of the MAP experiment in Sec. IV, comparing with previous calculations, and test the accuracy of our approximate power spectrum calculation. Finally, Sec. V discusses the potential speed of our method, likelihood estimation, mapping between the sets of parameters, accuracy, and systematic errors. The first appendix summarizes an analysis pipeline going from a measured power spectrum to cosmological parameter error estimates; the second appendix details several numerical difficulties with using the CMBFAST code for the calculations in this paper, along with suggested fixes.

Other recent attempts to speed up power spectrum computation through approximations include the dASH numerical package [23] and interpolation schemes [12]. Our method has the advantage of conceptual simplicity and ease of use combined with great speed and high accuracy.

II. COSMOLOGICAL PARAMETERS AND PHYSICAL QUANTITIES

We consider the standard class of inflation-like cosmological models, specified by five parameters determining

the background homogeneous spacetime (matter density Ω_{mat} , radiation density Ω_{rad} , vacuum energy density Ω_{Λ} , baryon density Ω_b , and Hubble parameter h), four parameters determining the spectrum of primordial perturbations (scalar and tensor amplitudes A_S and A_T and power law indices n and n_T), and a single parameter τ describing the total optical depth since reionization. We neglect additional complications such as massive neutrinos or a varying vacuum equation of state. This generic class of simple cosmological models appears to be a very good description of the Universe on large scales, and has the virtue of arising naturally in inflationary cosmology. Of course, any analysis of new data should first test whether this class of models actually provides an acceptably good fit to the data, and only then commence with determinations of cosmological parameters.

What constraints do a measurement of the microwave background power spectrum place on this parameter space? A rough estimate assumes the likelihood of a particular set of parameters is a quadratic function of the parameters (the usual Fisher matrix technique); better is a Monte-Carlo exploration of parameter space in the region of a best-fit model. For either technique to give reliable results, it is imperative to isolate the physical quantities which affect the microwave background spectrum and understand their relation to the cosmological parameters. If a set of physical quantities which have essentially orthogonal effects on the power spectrum can be isolated, then extracting parameter space constraints becomes much more reliable and efficient.

The five parameters describing the background cosmology induce complex dependences in the microwave background power spectrum through multiple physical effects. Using the physical energy densities $\Omega_{\text{mat}}h^2$, $\Omega_b h^2$, and $\Omega_{\Lambda} h^2$, as has been done in numerous prior analyses, improves the situation but is still not ideal. The characteristic physical scale in the power spectrum is the angular scale of the first acoustic peak, so it is advantageous to use this scale as a parameter which can be varied independently of any other parameters. This angular scale is in turn determined by the ratio of the comoving sound horizon at last scattering (which determines the physical wavelength of the acoustic waves) to the angular diameter distance to the surface of last scattering (which determines the apparent angular size of this yardstick). We first determine this quantity in terms of the cosmological parameters, and then choose three other comple-

mentary quantities. The analytic theory underlying any such choice of physical parameters has been worked out in detail (see [24, 25, 26, 27], and also [28, 29]).

The angular diameter distance to an object at a redshift z is defined to be $D_A(z) = R_0 S_k(r)/(1+z)$ where, following the notation of Peacock [30], R_0 is the (dimensionful) scale factor today and

$$S_k(r) = \begin{cases} \sin r, & \Omega > 1; \\ r, & \Omega = 1; \\ \sinh r, & \Omega < 1; \end{cases} \quad (1)$$

the Friedmann equation provides the connection between redshift z and coordinate distance r . With a dimensionless scale factor a and a Hubble parameter $H = \dot{a}/a$, the differential relation is

$$H_0 R_0 dr = \frac{-da}{[(1-\Omega)a^2 + \Omega_{\Lambda}a^4 + \Omega_{\text{mat}}a + \Omega_{\text{rad}}]^{1/2}}. \quad (2)$$

Thus the relation between scale factor and coordinate distance becomes

$$r = |\Omega - 1|^{1/2} \times \int_a^1 \frac{dx}{[(1-\Omega)x^2 + \Omega_{\Lambda}x^4 + \Omega_{\text{mat}}x + \Omega_{\text{rad}}]^{1/2}} \quad (3)$$

and the angular diameter distance is just

$$D_A(a) = aH_0^{-1}|\Omega - 1|^{-1/2}S_k(r), \quad (4)$$

using the above expression for r . Here we have used the relation $H_0 R_0 = |\Omega - 1|^{-1/2}$ which follows directly from the Friedmann equation.

The sound horizon is defined, in analogy to the particle horizon, as

$$r_s(t) = \int_0^t \frac{c_s(t')}{a(t')} dt' \quad (5)$$

where $c_s(t)$ is the sound speed of the baryon-photon fluid at time t ; to a very good approximation, before decoupling the sound speed is given by [24]

$$c_s^2 = \frac{1}{3} (1 + 3\rho_b/4\rho_{\gamma})^{-1}. \quad (6)$$

Using this expression plus the equivalent expression to Eq. (2) connecting dt and da gives

$$r_s(a) = \frac{1}{H_0\sqrt{3}} \int_0^a \frac{dx}{\left[\left(1 + \frac{3\Omega_b}{4\Omega_{\gamma}}x\right) \left((1-\Omega)x^2 + \Omega_{\Lambda}x^4 + \Omega_{\text{mat}}x + \Omega_{\text{rad}}\right)\right]^{1/2}}. \quad (7)$$

The physical quantity relevant to the microwave back-

ground power spectrum is

$$\mathcal{A} \equiv \frac{r_s(a_*)}{D_A(a_*)} \quad (8)$$

where the two functions are given by Eqs. (7) and (4), and a_* is the scale factor at decoupling. An accurate analytic fit for a_* in terms of the cosmological parameters has been given by Hu and Sugiyama [26]:

$$\begin{aligned} z_* &= \frac{1}{a_*} - 1 = 1048 [1 + 0.00124(\Omega_b h^2)^{-0.738}] \\ &\quad \times [1 + g_1(\Omega_{\text{mat}} h^2)^{g_2}], \quad (9) \\ g_1 &\equiv 0.0783(\Omega_b h^2)^{-0.238} [1 + 39.5(\Omega_b h^2)^{0.763}]^{-1}, \\ g_2 &\equiv 0.560 [1 + 21.1(\Omega_b h^2)^{1.81}]^{-1}. \end{aligned}$$

This fit applies to standard thermodynamic recombination for a wide range of cosmological models. (Note that while the formula was constructed only for models with the standard value for Ω_{rad} , the effect of a change of radiation density will come only through the redshift of matter-radiation equality, and thus $\Omega_{\text{mat}} h^2$ can be replaced by a factor proportional to $\Omega_{\text{mat}}/\Omega_{\text{rad}}$ to account for a variation in the radiation density. The changes in z_* are small anyway and have little impact on our analysis.) Since $a_* \ll 1$, the term proportional to Ω_Λ in Eq. (7) may be dropped and the integral performed, giving [25]

$$\begin{aligned} r_s(a) &= \frac{2\sqrt{3}}{3}(\Omega_0 H_0^2)^{-1/2} \left(\frac{a_{\text{eq}}}{R_{\text{eq}}}\right)^{1/2} \\ &\quad \times \ln \frac{\sqrt{1+R} + \sqrt{R+R_{\text{eq}}}}{1 + \sqrt{R_{\text{eq}}}}. \quad (10) \end{aligned}$$

where $R = 3\rho_b/4\rho_\gamma$ is proportional to the scale factor.

If two cosmological models are considered which both have adiabatic perturbations and the same value for \mathcal{A} , to high accuracy their acoustic peaks will differ only in height, not position. This is an obvious advantage for constraining models. The peak positions, and thus \mathcal{A} , will be extremely well constrained by power spectrum measurements. Other combinations which vary the peak heights only will be less well determined.

Choosing four other parameters describing the background cosmology must balance several considerations: (1) the new set of parameters must cover a sufficiently large region of parameter space; (2) the power spectrum should vary linearly or in some other simple way with the new parameters; (3) the new parameters should be nearly orthogonal in the cosmological parameter space; (4) the new parameters should correspond to the most important independent physical effects determining the power spectrum; (5) common theoretical prior constraints, like flatness or standard radiation, should be simple to implement by fixing a single parameter. No parameter set can satisfy all of these constraints perfectly. We use the following parameters, which provide a good balance between these criteria:

$$\begin{aligned} \mathcal{B} &\equiv \Omega_b h^2, \\ \mathcal{V} &\equiv \Omega_\Lambda h^2, \\ \mathcal{R} &\equiv \frac{a_* \Omega_{\text{mat}}}{\Omega_{\text{rad}}}, \end{aligned}$$

$$\mathcal{M} \equiv (\Omega_{\text{mat}}^2 + a_*^{-2} \Omega_{\text{rad}}^2)^{1/2} h^2. \quad (11)$$

\mathcal{B} is proportional to the baryon-photon density and thus determines the baryon driving effect on the acoustic oscillations [24, 27]. \mathcal{R} is the matter-radiation density ratio at recombination, which determines the amount of early Integrated Sachs-Wolfe effect. \mathcal{V} determines the late-time Integrated Sachs-Wolfe effect arising from a late vacuum-dominated phase, but otherwise represents a nearly exact degeneracy (sometimes called the ‘‘geometrical degeneracy’’). \mathcal{M} couples only to other small physical effects and is an approximate degeneracy direction. This choice of parameters is not unique, but this set largely satisfies the above criteria.

Given values for \mathcal{A} , \mathcal{B} , \mathcal{V} , \mathcal{R} , and \mathcal{M} , they can be inverted to the corresponding cosmological parameters by rewriting the definition of \mathcal{A} in terms of \mathcal{B} , \mathcal{V} , \mathcal{R} , \mathcal{M} , and h , then searching in h until the desired value for \mathcal{A} is obtained. Ω_b and Ω_Λ then follow immediately, while Ω_{mat} and Ω_{rad} can be obtained with a few iterations to determine a precise value for a_* . A less efficient but more straightforward method we have implemented is simply to search the 5-dimensional cosmological parameter space for the correct values.

The other cosmological parameters which affect the microwave background power spectrum, aside from tensor perturbations, are the reionization redshift and the amplitude and power law index of the scalar perturbation power spectrum. For reionization, we use the physical parameter

$$\mathcal{Z} \equiv e^{-2\tau}, \quad (12)$$

the factor by which the microwave background anisotropies at small scales are damped due to Compton scattering by free electrons after the Universe is reionized. At large scales, the temperature fluctuations are suppressed by a smaller amount.

The primordial perturbation amplitude cannot be measured directly, but only the amplitude of the microwave background fluctuations. Some care must be taken in the definition of the amplitude of the microwave fluctuations so that the other physical parameters are not significantly degenerate with a simple change in normalization. For example, one common normalization is some weighted average of the C_l 's over the smallest l values, say $2 < l < 20$ [31]. This is known as ‘‘COBE-normalization’’ because this is the range of scales probed by COBE, which tightly constrains the normalization of the temperature fluctuations at these scales [11]. But although such a normalization is useful for interpreting the COBE results, it is a bad normalization to adopt when probing a much larger range in l -space. The reason is that the lowest multipoles have a significant contribution from the Integrated Sachs-Wolfe effect: if the total matter density changes significantly between two models, the resulting low l multipole moments will also change. If the normalization is fixed at low l , then the result is that the two models will be offset at high l values. As a

concrete example, consider two models which differ only in \mathcal{V} , with \mathcal{A} , \mathcal{B} , \mathcal{M} and \mathcal{R} held fixed. The only physical difference between these two models is a difference in the structure growth rate at low redshifts, and in particular the fluctuations at the last scattering surface are identical. But if these two models are COBE normalized, then every C_l for $l = 20$ is offset between the two models. Defining the normalization as an average band power over a wider range of l values [10] is better but not ideal. We advocate defining a normalization parameter \mathcal{S} by the amplitude of the perturbations on the scale of the horizon at last scattering, corrected by the amount of small-scale suppression in the C_l 's due to reionization. In practice, for models with the same values of n , this normalization essentially corresponds to the amplitude of the acoustic oscillations at l values higher than the first several peaks. Note that increasing \mathcal{Z} while holding \mathcal{S} and the other physical parameters fixed keeps the microwave background power spectrum the same at high l while enhancing the signal at low l . The first few peaks cannot be used for normalization because they have been subjected to driving by the gravitational potential as they cross the horizon [27], so their amplitudes vary significantly with \mathcal{B} and \mathcal{R} , as shown in the following Section.

The primordial power spectrum of density perturbations is generally taken to be a power law, $P(k) \propto k^n$, with $n = 1$ corresponding to the scale-invariant Harrison-Zeldovich spectrum. Making the approximation that k and l have a direct correspondence, the effect of n on the microwave background power spectrum can be modelled as

$$C_l(n) = C_l(n_0) \left(\frac{l}{l_0} \right)^{n-n_0}, \quad (13)$$

which is a good approximation for power law power spectra. A departure from a power law, characterized by α [32], can be represented in a similar way. Note that since the dependence is exponential, a linear extrapolation is never a good approximation over the entire interesting range $2 < l < 3000$. The choice of l_0 is arbitrary: changing l_0 simply gives a different overall normalization.

Finally, note that the amplitude of the tensor mode power spectrum should be used as a separate parameter, not the common choice of the tensor-scalar ratio. The tensor modes contribute at comparatively large angular scales; they are significant only for $l < 100$ given current rough limits on the tensor amplitude. Varying the tensor amplitude independently automatically leaves the normalization parameter \mathcal{S} fixed.

In the rest of the paper, we refer to the parameters \mathcal{A} , \mathcal{B} , \mathcal{V} , \mathcal{R} , \mathcal{M} , \mathcal{S} , and \mathcal{Z} as “physical parameters”, as opposed to the usual “cosmological parameters” Ω_b , Ω_{mat} , Ω_{rad} , Ω_{vac} , h , Q^2 (a quadrupole-based normalization), and z_r .

III. POWER SPECTRA

We now present the dependence of the temperature fluctuation power spectrum on these physical parameters. As a fiducial model, we choose a standard cosmology with $\Omega = 0.99$, $\Lambda = 0.7$, $\Omega_{\text{mat}} = 0.29$, $\Omega_b = 0.04$, $h = 0.7$, $n = 1$, and full reionization at redshift $z_r = 7$, with standard neutrinos. We compute power spectra for the fiducial model and for evaluating the various numerical derivatives using Seljak and Zaldarriaga’s CMBFAST code [33, 34, 35]. Note that the model is slightly open rather than flat to compensate for numerical instabilities in the CMBFAST code; see the discussion in the Appendix. The corresponding physical parameters are $\mathcal{A}_0 = 0.0106$, $\mathcal{B}_0 = 0.0196$, $\mathcal{V}_0 = 0.338$, $\mathcal{M}_0 = 0.154$, and $\mathcal{R}_0 = 3.252$. Since the dependence of the spectrum on \mathcal{S} is trivial, its definition is arbitrary; it can be taken, for example, as the amplitude of a particular high peak, or as the equivalent scalar perturbation amplitude A_S at the scale which the power law n is defined for a model with no reionization. We do not consider tensor perturbations in this paper, which can be analyzed separately by the same techniques; the tensor perturbations are simpler because they depend on fewer parameters than the scalar perturbations. None of the following results depend qualitatively on the fiducial model chosen.

The top panel of Fig. 1 displays power spectra as the parameter \mathcal{A} varies while the other physical parameters are held fixed. It is clear that the effect of \mathcal{A} is *only* to determine the overall angular scale, except for the small Integrated Sachs-Wolfe effect for $l < 200$. For the bottom panel, the l -axis of each power spectrum is rescaled to give C_l as a function of $l\mathcal{A}/\mathcal{A}_0$, and then the percent difference between the rescaled model and the fiducial model is plotted. The small variation of the scaled power spectrum between around $l = 50$ and $l = 200$ is due to the early ISW effect and can be accurately modelled as a linear variation, while between $l = 2$ and $l = 50$ the variation with \mathcal{A} is more complicated due to the late-time ISW contribution. For $l > 200$, the scaled power spectra match to within 1%; the residual discrepancy is likely due to numerical inaccuracy. Since \mathcal{A} will be tightly constrained by the peak positions, this numerical error will not affect the determination of \mathcal{A} , but may contribute a systematic error to the determination of other parameters at the 1% level.

Figure 2 displays the power spectrum variation with \mathcal{B} , keeping the other parameters fixed. This plot clearly shows the well-known baryon signature of alternating peak enhancement and suppression. The variation of a particular multipole C_l with \mathcal{B} is highly linear for $l > 50$ for variations of up to 20%; for all multipoles, the dependence is linear for variations of up to 10%. A figure of merit for a linear approximation to the power spectrum is whether the errors in the approximation are negligible compared to the cosmic statistical error at a given multipole. The bottom panel of Fig. 2 shows just how good the linear approximation is for several selected l values. The

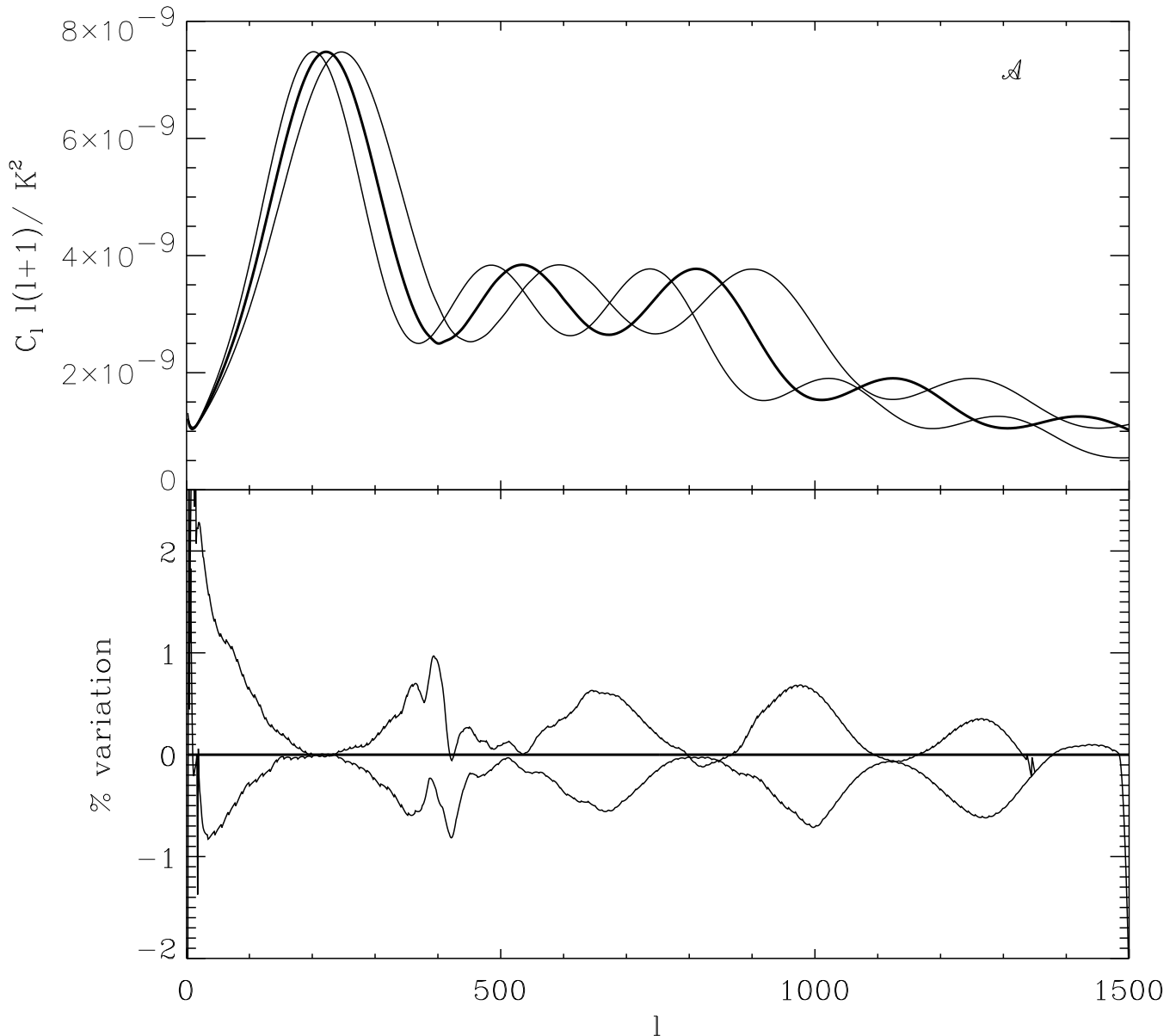


FIG. 1: Temperature power spectra for the fiducial cosmological model (top panel, heavy line), plus models varying the parameter \mathcal{A} upwards by 10% (curve shifts to lower l values) and downwards by 10% (curve shifts to higher l values) while keeping \mathcal{B} , \mathcal{M} , \mathcal{V} , \mathcal{R} , \mathcal{S} and n fixed. The bottom panel displays the fractional error between the fiducial model and the other two models with l -axes rescaled by the factor $\mathcal{A}/\mathcal{A}_r$.

horizontal axis plots the fractional change in the parameter \mathcal{B} . The vertical axis plots the ratio of the change in C_l , $C_l(B) - C_l(B_0)$, to the statistical error from the cosmic variance at that multipole, $\sigma_l = C_l(B_0)\sqrt{2/(2l+1)}$. (Any measurement of the multipole C_l is subject to a statistical error at least as large as this cosmic variance error, due to the finite number of modes sampled on the

sky.) The linear dependence remains valid even near the “pivot” points between a peak and a trough. Thus a linear extrapolation using computed numerical derivatives is highly accurate at reproducing the \mathcal{B} dependence; the error in such an approximation appears to be dominated by systematic numerical errors in computing the power spectrum, and funny behavior of some of the multipoles

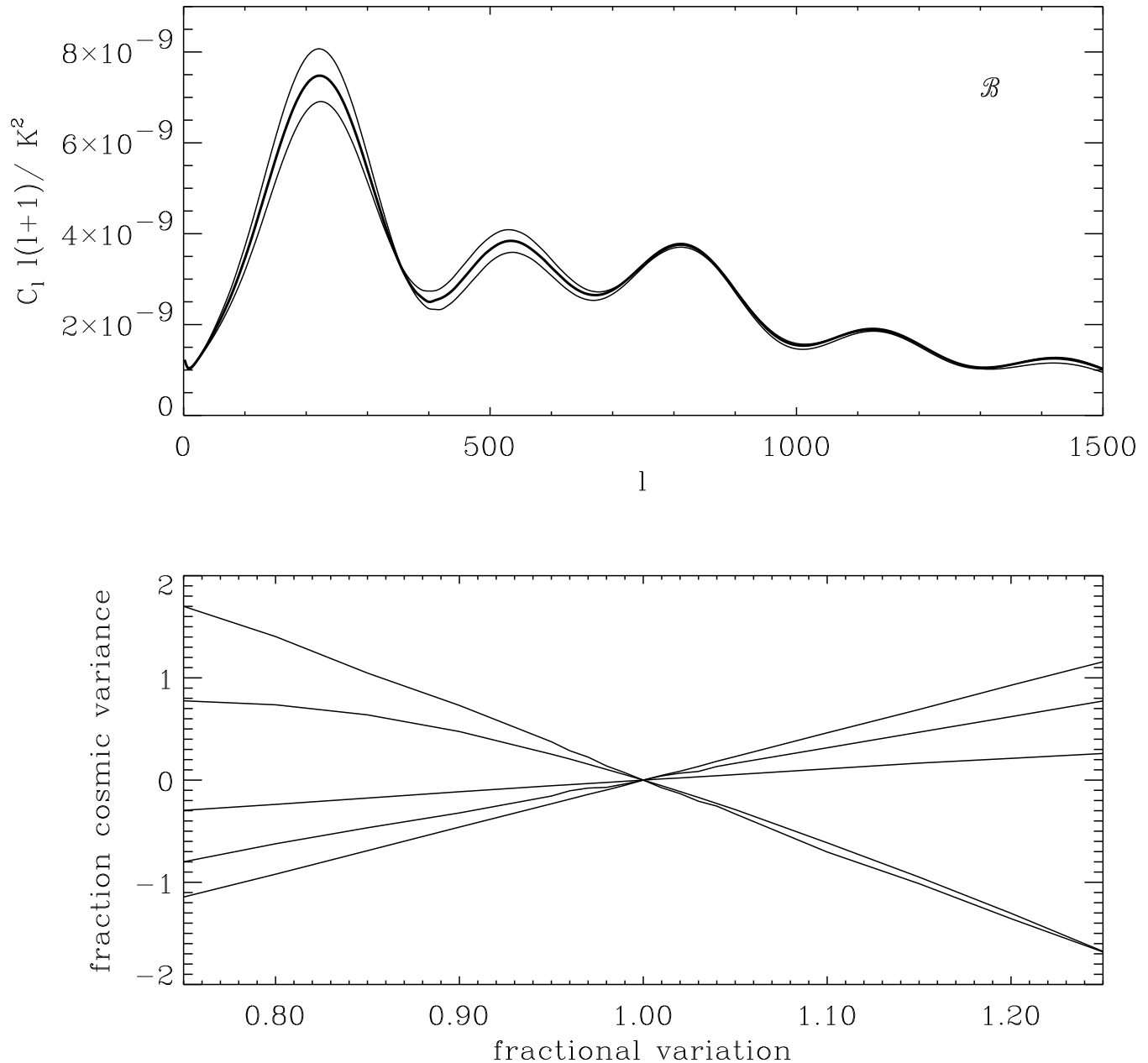


FIG. 2: Temperature power spectra for the fiducial cosmological model (top panel, heavy line), plus models varying the parameter \mathcal{B} upwards by 25% (higher first peak) and downwards by 25% (lower first peak) while keeping \mathcal{A} , \mathcal{M} , \mathcal{V} , \mathcal{R} , \mathcal{S} , and n fixed. The bottom panel displays C_l as a function of \mathcal{B} , for $l = 50, 100, 200, 500$, and 1000 . The horizontal axis shows the fractional change in \mathcal{B} , while the vertical axis gives the change in C_l as a fraction of the cosmic variance at that multipole.

for small variations in \mathcal{B} is surely due to systematic errors.

Figure 3 shows the variation of the power spectrum with respect to the parameter \mathcal{R} , keeping the others fixed, with the corresponding dependence of specific multipoles. For smaller values of \mathcal{R} , matter-radiation equality occurs later, so the Universe is less accurately de-

scribed as matter-dominated at the time of last scattering, leading to an increased amplitude of the first few peaks from the Integrated Sachs-Wolfe effect at early times. The dependence on \mathcal{R} is not quite as linear as for \mathcal{B} , but still the spectrum varies highly linearly with \mathcal{R} for parameter variations of 10% for $l > 30$. Figure 4 shows the same for the parameter \mathcal{M} , which is an approx-

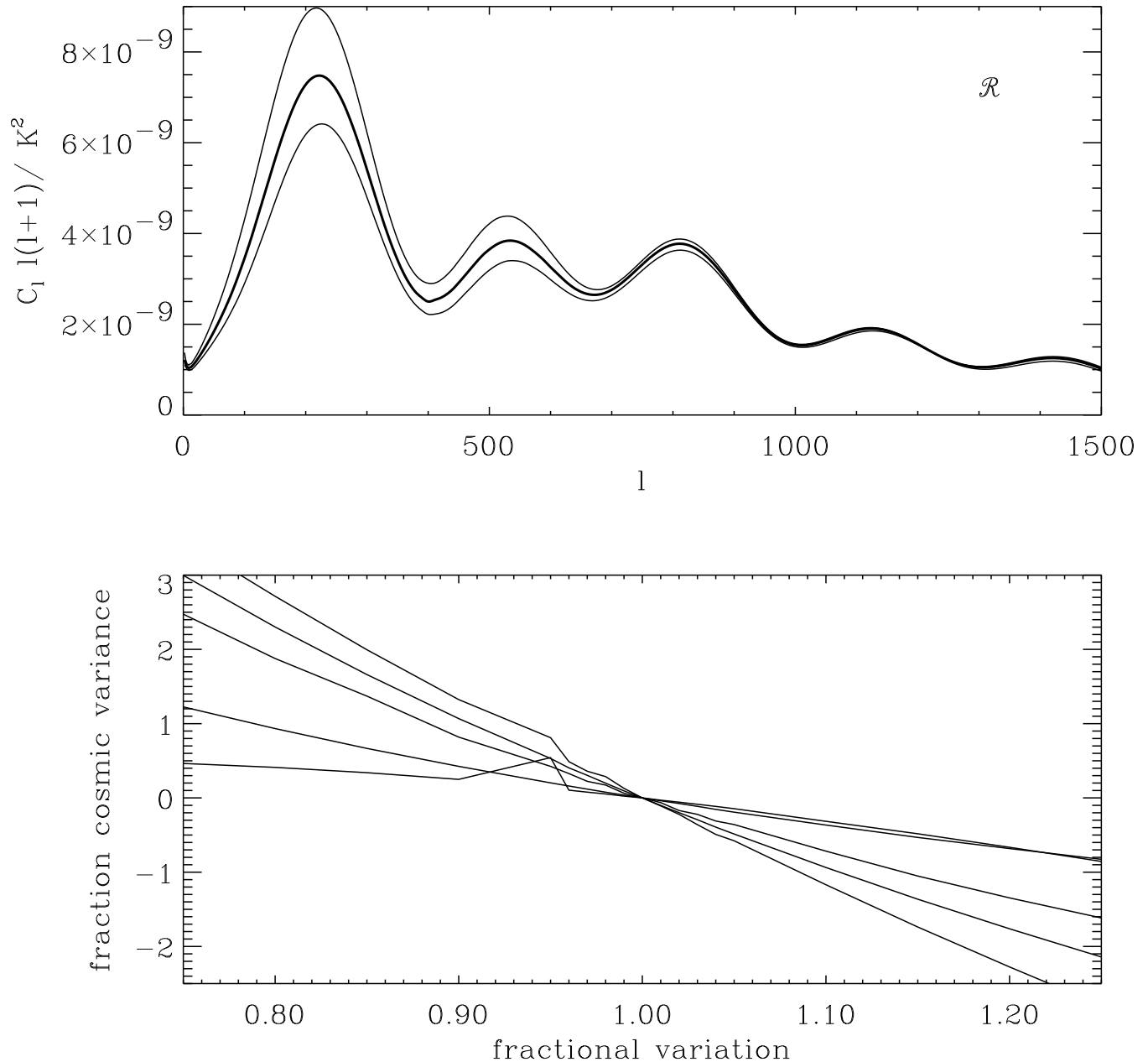


FIG. 3: Same as Fig. 2, except varying the parameter \mathcal{R} while keeping the others fixed. Larger \mathcal{R} increases the peak heights. The substantial glitch in the bottom panel is due to systematic errors in CMBFAST.

imate degeneracy direction: the power spectrum changes noticeably only in the neighborhood of the first peak. If the standard three massless neutrino species is imposed as a prior, \mathcal{M} is fixed.

Variation of \mathcal{V} holding the others fixed is nearly an exact physical degeneracy [9, 10], broken only by the late-time ISW effect at low multipole moments displayed in Fig. 5. This variation at small l values is not well approximated by simple linear extrapolation; accurate approx-

imation must rely on more sophisticated schemes, but the total contribution to constraining cosmological models will have comparatively little weight due to the large cosmic variance. At higher l values, the power spectra should be precisely degenerate, and the extent to which they are not is a measure of numerical inaccuracies. Note that the inaccuracies are in the form of systematic offsets at levels smaller than a percent. When analyzing data, the variation in \mathcal{V} can simply be set to zero for all l val-

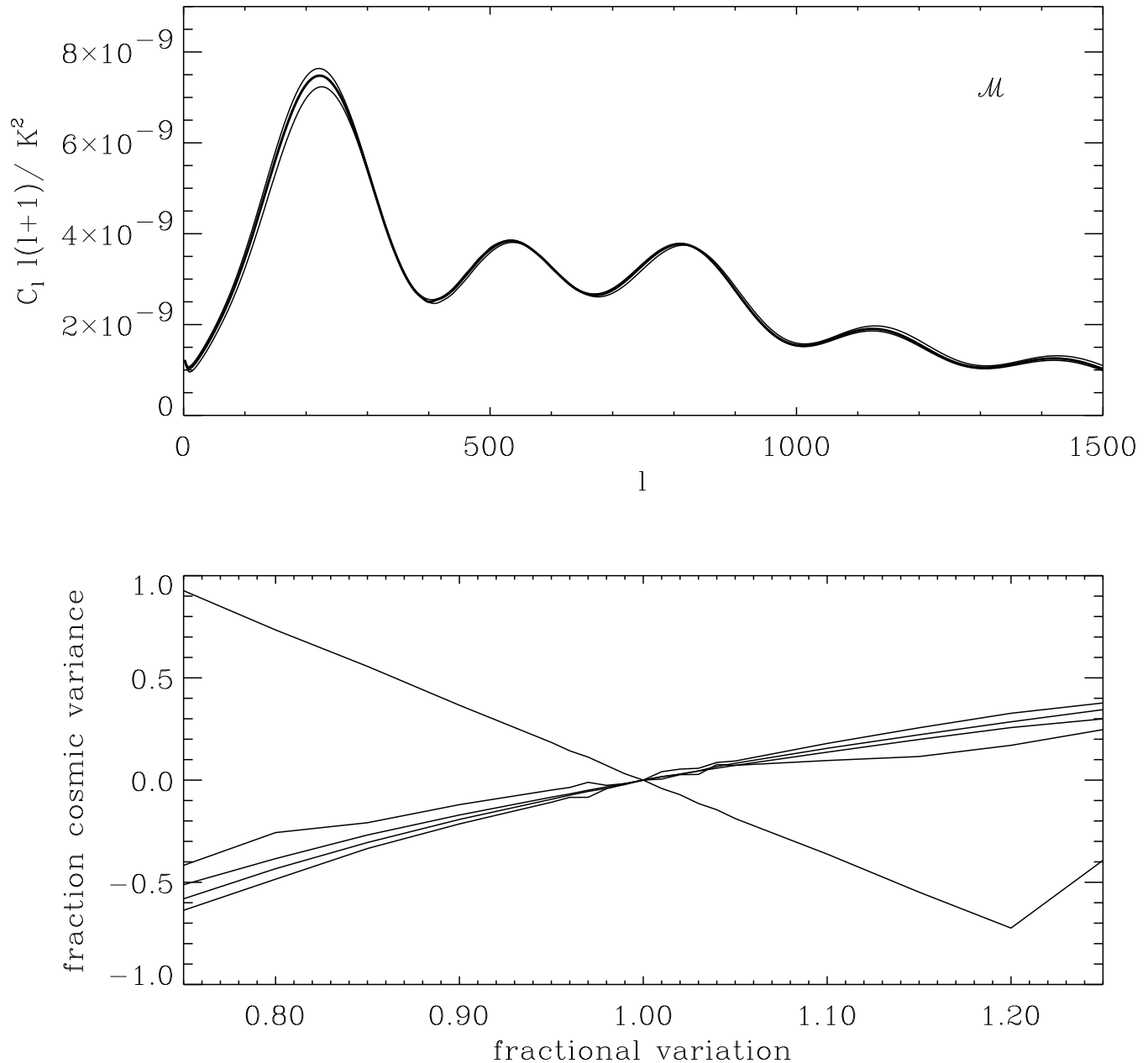


FIG. 4: Same as Fig. 2, except varying the parameter \mathcal{M} while keeping the others fixed. Larger \mathcal{M} increases the first peak height. Again, the glitch in the bottom panel is due to systematic errors in CMBFAST.

ues higher than the first acoustic peak. If a flat universe is imposed as a prior condition, the parameter \mathcal{V} is then fixed.

Aside from initial conditions, reionization is the other physical effect which can have a significant impact on the power spectrum. Note that the effective normalization we use depends on \mathcal{Z} , so that as \mathcal{Z} varies, the power spectrum retains the same amplitude at high l . As discussed in the previous section, for large l the effect of chang-

ing the total optical depth is effectively just a change in the overall amplitude. Thus for our set of parameters, variations in \mathcal{Z} while holding the other parameters fixed change the power spectrum only at the largest scales. For this reason, we do not consider reionization further here. Note that for polarization, reionization will generate a new peak in the polarization power spectrum at low l , and this effect may require more complicated analytic modelling than a simple linear extrapolation [36].

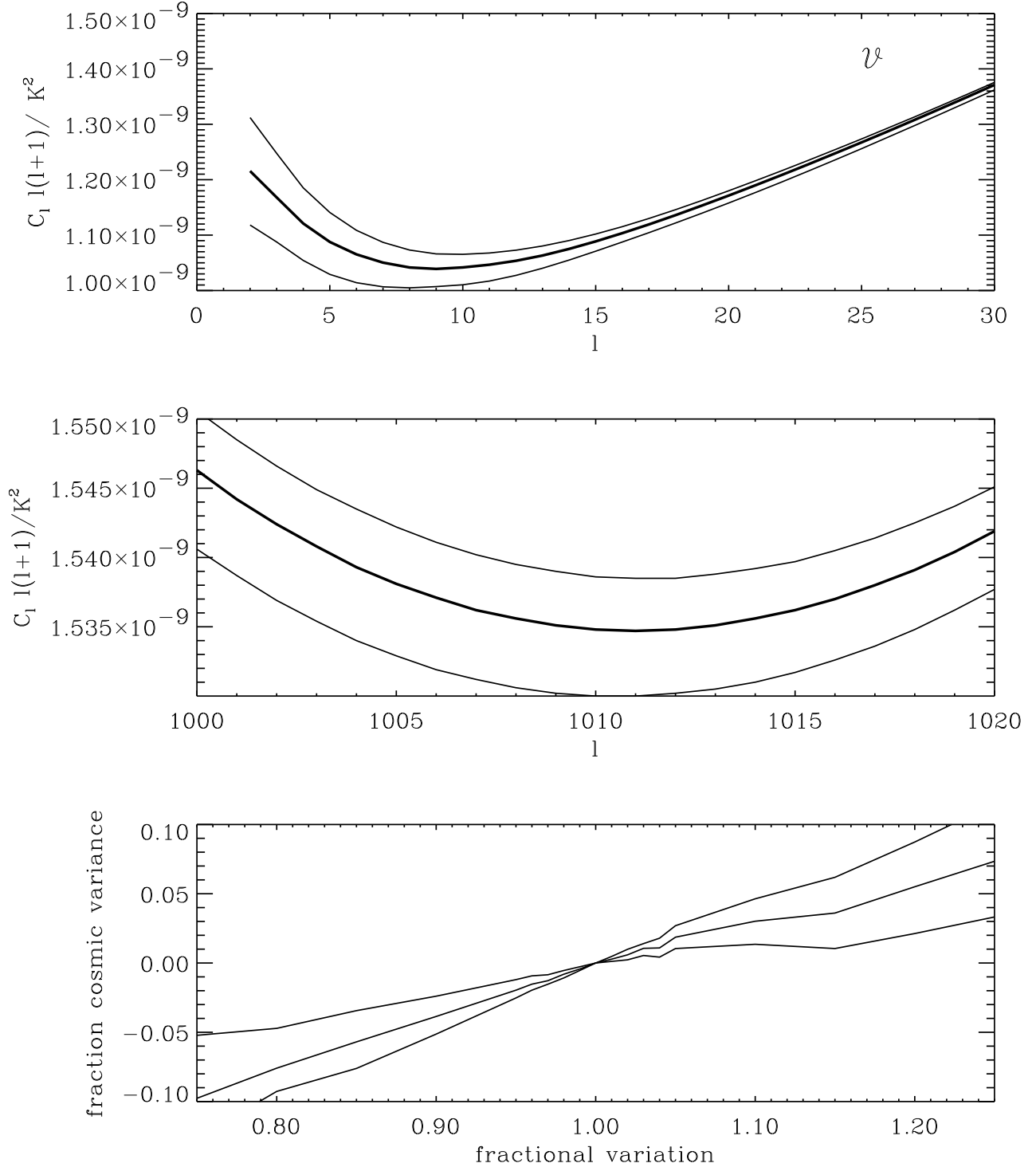


FIG. 5: Varying the the parameter \mathcal{V} , keeping the others fixed, for low l (top) and higher l (center) values; note the scales of the vertical axes. Only the lowest multipoles have any significant variation, arising from the Integrated Sachs-Wolfe effect at late times; the bottom panel shows the dependence of the $l = 5, 10,$ and 20 multipoles on \mathcal{V} . A linear approximation is rough but reasonable; higher-order approximations will model this dependence better. At higher l , the variation between the curves is a measure of the numerical accuracy of the code generating the C_l curves.

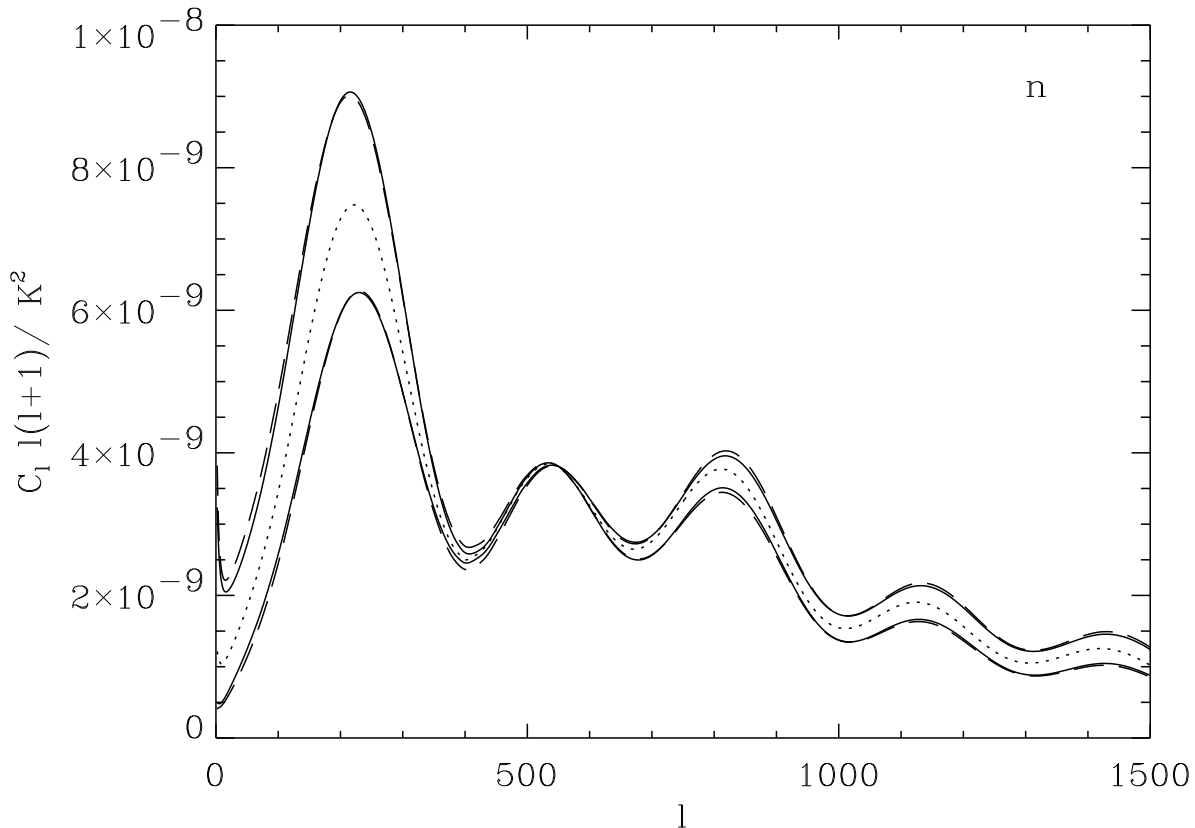


FIG. 6: A comparison of computed (solid) and approximated (dashed) power spectra for different values of the scalar index n , for $n = 0.8$ and $n = 1.2$ (dashed), where the approximated values have been calculated by applying Eq. (13) to the $n = 1$ model (dotted). Note the displayed variation in n is roughly three times larger than the constraint MAP will impose (see Fig. 7).

Finally, we show the effect of changing the spectral index n of the primordial power spectrum in Fig. 6. Equation (13) gives a very good approximation to the effect of changing n ; the largest errors are at small l and in the immediate region of the first few peaks and troughs, amounting to less than 10% of the cosmic variance for any individual multipole.

We have now displayed simple numerical or analytic approximations for the effect of all parameters with a sizeable impact on the cosmic microwave background power spectrum, for $l > 50$ and for parameter variations which are in the range to which the parameters will be restricted by upcoming microwave background maps. For a model which differs from a fiducial model in several different parameters, it is in principle ambiguous in what order to do the various extrapolations and approximations. For example, should a reionization correction be applied before or after the \mathcal{A} parameter extrapolation? In practice, however, most of the parameter ranges involved will be quite small, particularly for the \mathcal{A} parameter, and the order in which all of the approximations are applied to the fiducial spectrum is essentially irrelevant. We test the validity of the various approximations for arbitrary

models below.

We also note that while we have demonstrated explicitly the validity of linear extrapolations and other simple approximations in computing deviations from a particular fiducial power spectrum, we have not shown explicitly that this is true for any fiducial cosmological model. But current measurements point towards a Universe well-described by a model close to the fiducial one considered here, and in the unlikely event that the actual cosmology is significantly different, the various approximations are simple to check explicitly for any underlying model.

Some of the linear extrapolations lose accuracy for the smallest l values. It is not clear whether any simple approximation is sufficient for reproducing the power spectrum for small l values, because a variety of different effects contribute in varying proportions. While these large scales have significant cosmic variance and do not have very much statistical weight compared to the rest of the spectrum, several parameters (\mathcal{V} , \mathcal{Z} , \mathcal{T} , n_T) have significant effects *only* at small l , and accurate limits on these parameters will require approximating these moments. One possible approach is to use quadratic or higher-order extrapolations. We have not explored the

efficacy of such approximations, and they may require a more accurate numerical code, but promise to be a good solution. A more complicated approach would be to develop analytic fitting formulas. Steps in this direction have been taken by Durrer and collaborators [37], but their solutions rapidly lose accuracy for $l > 10$, and a variety of physical effects are neglected which contribute at the few percent level or more. Another possibility is an expanded numerical approximation, where the effects of our parameters are fit as linear or quadratic, but instead of fitting the total C_l dependence, the various separate terms (i.e., quadratic combinations of Sachs-Wolfe, Integrated Sachs-Wolfe, doppler, and acoustic effects) contributing to each C_l are modelled independently. In the estimates below, we will not consider tensor perturbations and fix the parameter \mathcal{Z} , while \mathcal{V} is a degenerate direction; we thus sidestep the issue of approximating the power spectrum for low l , and do not discuss the issue further here.

IV. ERROR REGIONS FOR COSMOLOGICAL PARAMETERS

Given some data, we want to determine the error region in parameter space corresponding to some certain confidence level in fitting the data. This must be done by looking around in parameter space in the vicinity of the best-fitting model. With a fast computation of the theoretical power spectrum for different points in parameter space in hand, a straightforward Metropolis algorithm can be used to construct a Monte-Carlo exploration of the parameter space. Refined techniques with the label of Markov Chains have recently been applied to the microwave background [15, 38]. Our approximate power spectrum evaluation renders these techniques highly efficient.

As a demonstration, we consider estimated power spectrum measurement errors drawn from the χ^2_{2l+1} probability distribution derived in Ref. [39]. We assume that the Universe is actually described by a particular fiducial cosmological model. With the simple assumption that the measurement errors for each C_l are uncorrelated, the likelihood of a cosmological model being consistent with a measurement of the fiducial model becomes trivial to compute. Then we map the likelihood around the fiducial model via a Markov Chain of points in parameter space, starting with the fiducial model and moving to a succession of random points in the space using a simple Metropolis-Hastings algorithm. Sophisticated convergence tests can be applied to the chain to determine when the distribution of models in the Monte Carlo has converged to a representation of the underlying likelihood function. The chain of models should be constructed in the physical parameter space: the roughly orthogonal effects of the physical parameters on the power spectrum leads to an efficient Monte Carlo sampling of the space. For each model in the chain, the cosmological param-

eters of the model are computed and stored along with the physical parameters.

The commonly-used Fisher matrix approximation [8] expands the likelihood function in a Taylor series around the most likely model and retains only the quadratic term. With Gaussian uncorrelated statistical errors, the Fisher matrix approximation becomes exact whenever the parameter dependence of the C_l 's is exactly linear in all parameters. Since the power spectrum is nearly linear in most of our physical parameter set, we can check our Monte Carlo results by comparing with the Fisher matrix likelihood computed with the physical variables.

As a simple illustration, we determine the error region corresponding to a simplified model of the power spectrum which will be obtained by the MAP satellite, currently collecting data. MAP's highest frequency channel has a gaussian beam with a full-width-half-max size of about 0.21 degrees. MAP will produce a full-sky map of the microwave background at this resolution with a sensitivity of around $35 \mu\text{K}$ per 0.3 square-degree pixel. We neglect eventual sky cuts and assume all C_l estimates are uncorrelated. We consider models with only scalar perturbations and fixed reionization. The physical parameter space is thus \mathcal{A} , \mathcal{B} , \mathcal{M} , \mathcal{R} , \mathcal{V} and n . The other parameters we have fixed (tensor perturbations, \mathcal{Z}) affect the power spectrum only at small l , and will have little effect on the physical parameters considered. We assume the underlying cosmology is described by the fiducial model of the previous section. Fundamental physical constraints have been enforced: $\Omega_b < \Omega_{\text{mat}}$ and all densities must be positive. Additionally, we only consider models with $\Omega_{\text{vac}} < 2$ and discard any models which are not invertible from the physical to the cosmological parameters (these amount to a handful of models with extreme parameter values).

Figure 7 shows the anticipated MAP error contours in the physical parameter space, extracted from a Markov Chain of 3×10^4 models. The full 7-dimensional likelihood region is projected onto all pairs of parameters. The parameter \mathcal{V} is essentially unconstrained by MAP, while \mathcal{M} has a $1-\sigma$ error of around 30%. Measurements extended to smaller scales will not significantly improve constraints on these two parameters: they represent true physical degeneracies in the model space. The other parameters are well constrained. Approximate $1-\sigma$ errors are: 0.5% for \mathcal{A} , 5% for \mathcal{R} , 3% for \mathcal{B} , 2% for \mathcal{S} , and 3% for n . The error regions are elliptical, because the likelihood region in these parameters is well-approximated by a quadratic form. The residual correlations involving \mathcal{S} and n will be lifted by measurements out to higher l values; the parameters are largely uncorrelated in their power spectrum effects. Figure 8 shows a Fisher matrix estimate of the same likelihood. The two sets of likelihood contours are very close, as expected since we have shown explicitly that the power spectrum varies nearly linearly in the physical variables over a parameter region consistent with MAP-quality data. The most notable exception is the variable \mathcal{A} , which does not give

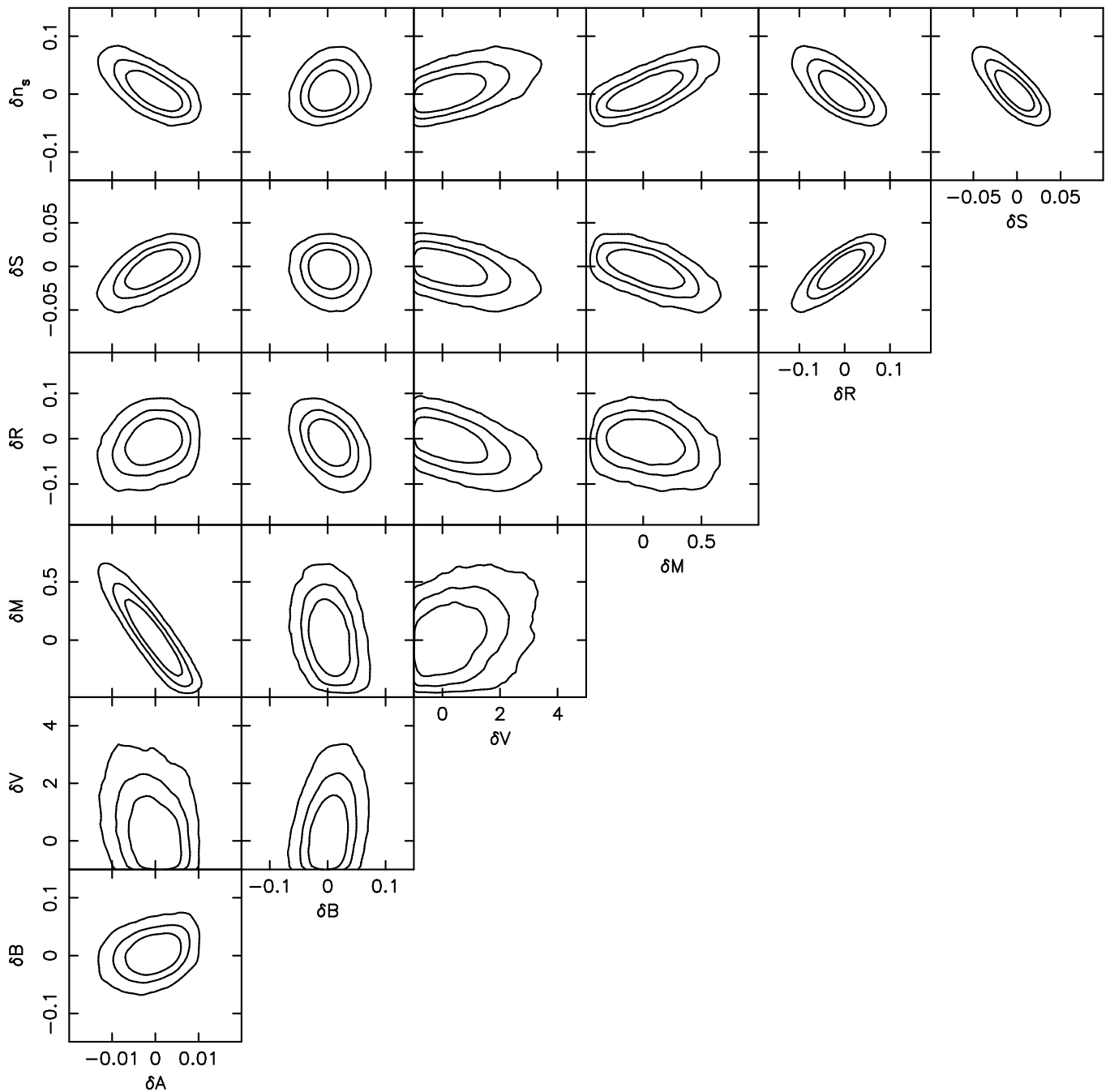


FIG. 7: Parameter error contours anticipated for the MAP satellite in the physical parameter space. In each panel, the entire likelihood region has been projected onto a particular plane. The axis refer to the fractional variation for each parameter with respect to the fiducial one, e.g. $\delta A = (A - A_{\text{fid}})/A_{\text{fid}}$. The contours show 68%, 95%, and 99% confidence levels.

a linear variation, but it is so well constrained that it is effectively fixed when considering its impact on determining the other parameters. The contours will also differ slightly due to the nonlinear behavior of n , but the general excellent agreement demonstrates that our Monte Carlo technique works as expected.

In Fig. 9, we replot Fig. 7 in the cosmological parameter space. This procedure is trivial, since we calculate the

cosmological parameter set for each model. The resulting contours are deformed, reflecting the non-linear relation between the physical and cosmological parameter sets. Clearly, a Fisher matrix approximation in the cosmological variables, as has been done in numerous analyses, will give significantly incorrect error regions [10]. Note, however, that for MAP-quality data, the Fisher matrix errors in the physical variables projected into the cosmo-

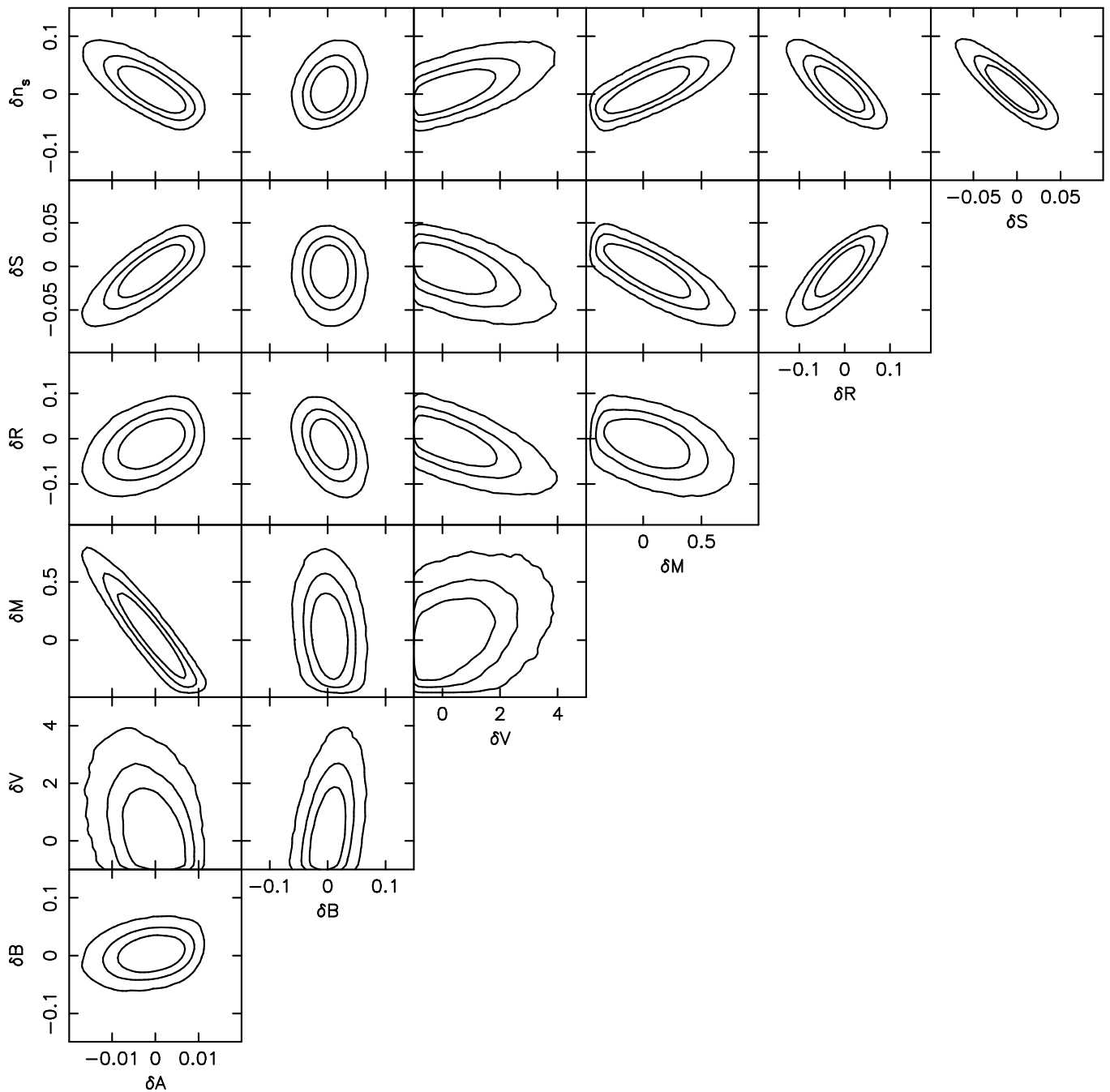


FIG. 8: The same as Fig. 7, except using the Fisher matrix approximation to the actual likelihood. The contours in the two cases are very similar.

logical variables gives a highly accurate result, Fig. 10, in contrast to the claims in Ref. [10]. The Fisher matrix approximation in the physical parameter space can be used to further increase the efficiency of error region evaluation, which may be useful in the cases where the computation of the error regions is dominated by evaluation of the likelihood for a given model from actual data. If the likelihood evaluation is at least as efficient as the power spectrum evaluation, then the increased efficiency from a

Fisher matrix approximation may not result in dramatic increases in computational speed, since in both cases the physical parameter space must be sampled and parameter conversion performed at each point to construct the likelihood contours in the space of the cosmological parameters.

It is useful to plot error regions in both sets of parameters. Physical parameters represent the actual physical quantities which are being directly constrained by the

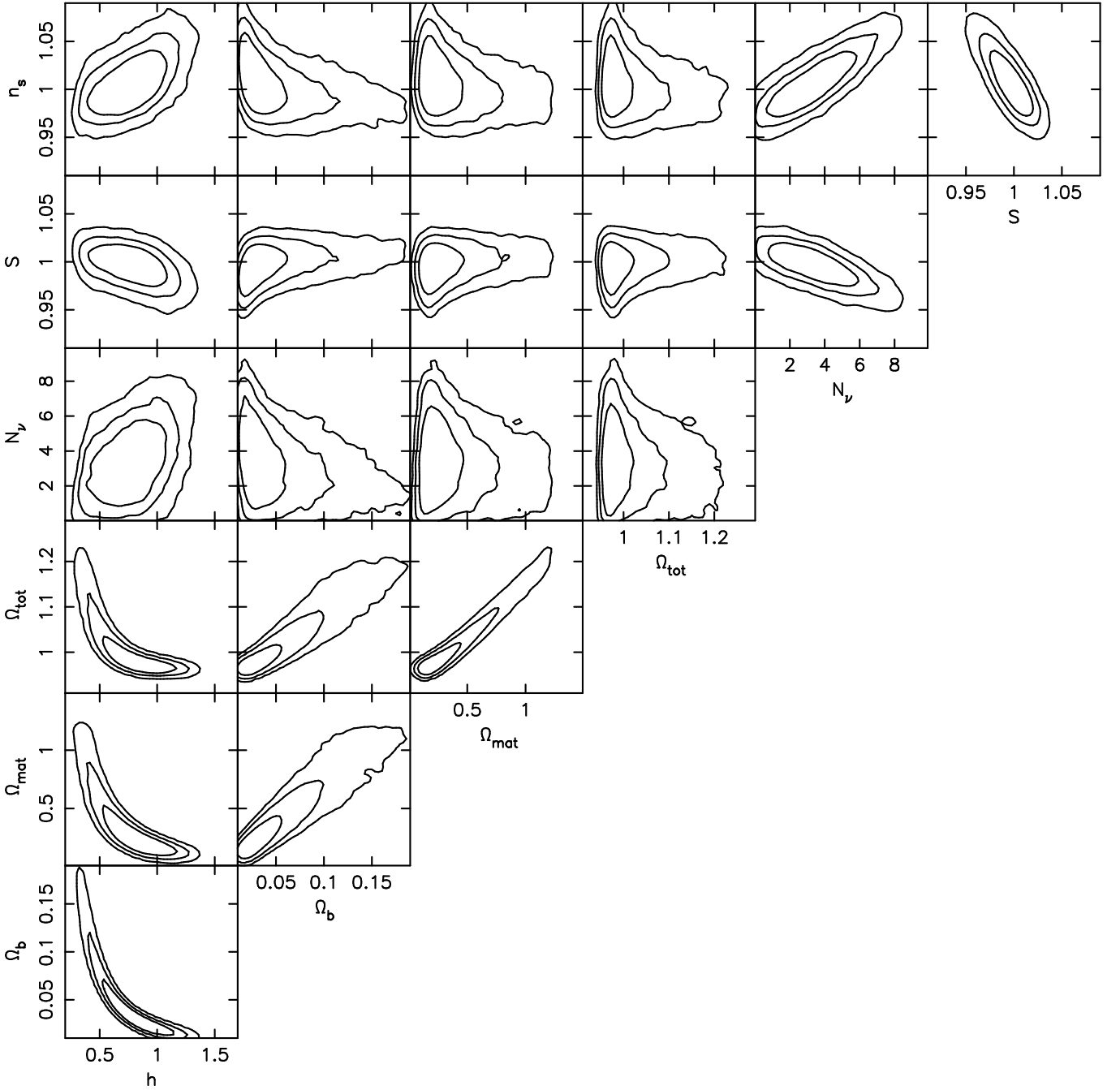


FIG. 9: The likelihood distribution in Fig. 7 mapped into the cosmological parameter space.

measurements, and the error regions are nearly elliptical. The cosmological parameters are useful theoretically and for comparisons with other data sources, i.e. large-scale structure or supernova standard candles. One advantage of determining the error region via a Monte Carlo technique is that prior constraints on cosmological parameters can be implemented simply.

When the Fisher matrix approximation is computed in the physical parameter space, it is highly accurate. This does not actually help much, however: if information

about cosmological parameters is desired, transforming from the physical to the cosmological parameter space requires some kind of sampling of the likelihood region. The most efficient way to do this is via Monte Carlo, so the additional computational overhead in performing a Monte Carlo likelihood evaluation of the physical variable likelihood instead of a Fisher matrix approximation is negligible.

To test the validity of our numerical power spectrum approximations, we choose 1000 models at random from

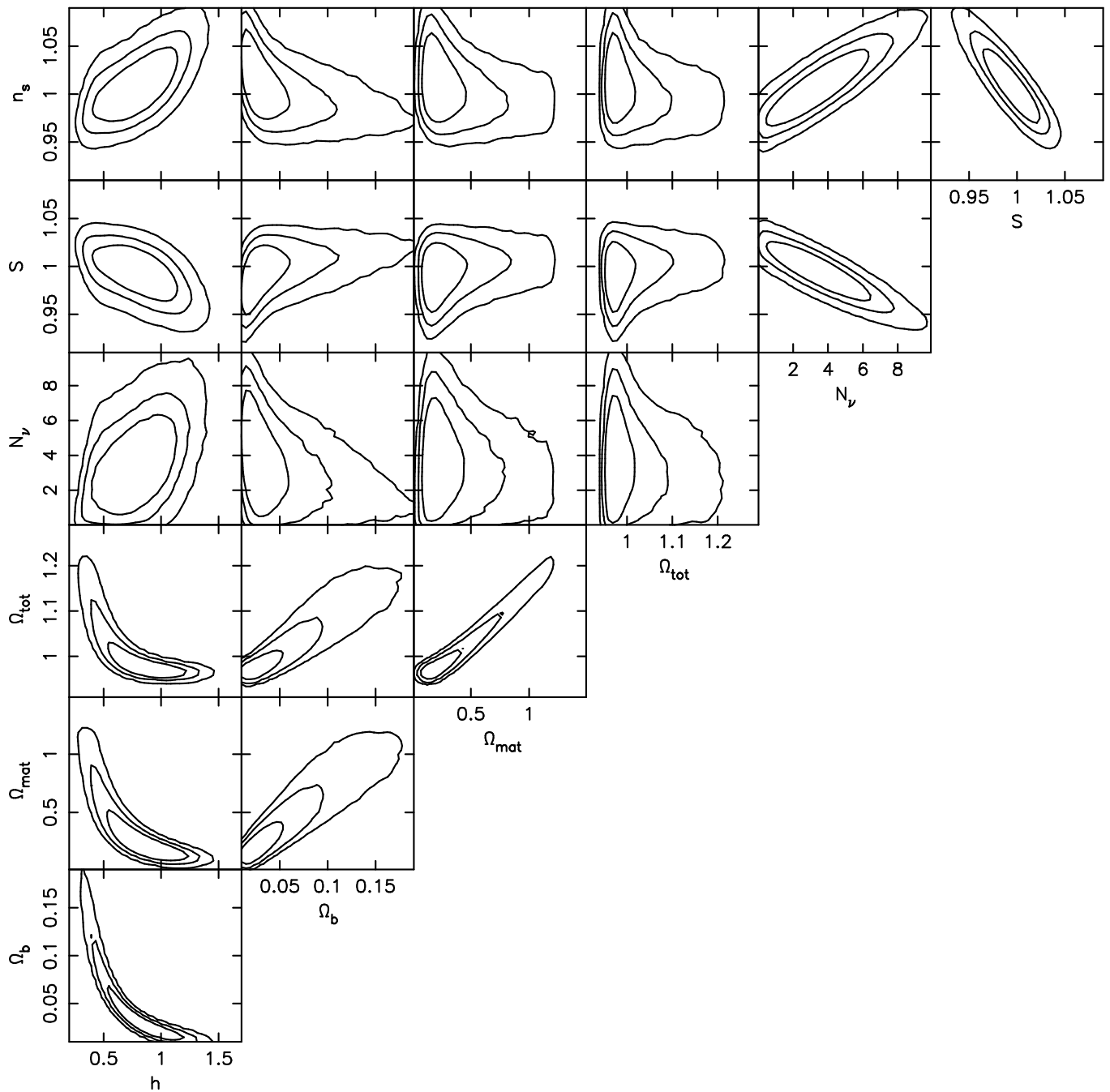


FIG. 10: The likelihood distribution in Fig. 8 mapped into the cosmological parameter space. These contours, derived from a Fisher matrix approximation, are very close to those in Fig. 9.

the above Monte Carlo set of cosmological models. We compute each numerically using CMBFAST, and then compare the computed and approximated models. The two are compared using the statistic

$$\chi^2 = \sum_l (C_l^{\text{approx}} - C_l^{\text{num}})^2 (\sigma_l^{\text{MAP}})^{-2} \quad (14)$$

where $(\sigma_l^{\text{MAP}})^2$ is the variance of C_l in our model MAP data. For MAP, the measured power spectrum will

consist of approximately 800 independent multipole moments, so an approximate power spectrum which differs from the actual model power spectrum by the MAP error at each multipole will have a value for the statistic χ^2 of around 800. Figure 11 shows the error distribution for our subset of models. The statistic χ^2 for each model is plotted against the “distance” in physical parameter space of the model from the fiducial model, where the

distance measure is the Fisher matrix:

$$d = [(\mathbf{P} - \mathbf{P}_0)F(\mathbf{P} - \mathbf{P}_0)]^{1/2}, \quad (15)$$

where \mathbf{P} is a vector of physical parameters corresponding to the model considered, \mathbf{P}_0 is the vector of fiducial-model parameters, and

$$F_{ij} = \sum_l \frac{1}{(\sigma_l^{\text{MAP}})^2} \frac{\partial C_l}{\partial P_i} \frac{\partial C_l}{\partial P_j} \quad (16)$$

is the Fisher matrix. This is roughly equivalent to measuring the distance along each axis in the physical parameter space in units of the $1\text{-}\sigma$ error interval in that parameter direction. The solid-circle points are models with $2 < N_\nu < 4$, for which the worst-approximated models disappear. The difference has two possible origins: either linear extrapolation is not valid over a large enough range in the variables \mathcal{R} and \mathcal{M} to handle these models, or CMBFAST does not provide accurate computations in this range. The second possibility seems more likely, since the code contains an explicit trap preventing computations for these unusual numbers of neutrino species.

For essentially all other models, the error averaged over all multipoles is small compared to the MAP statistical errors, and the error distribution is roughly independent of the distance in parameter space, showing that our numerical approximations are valid. Furthermore, most of the total error tends to come from a small number of multipoles, indicating that systematic errors in CMBFAST dominate the total difference between our approximations and the direct numerical calculations. Given this fact, we forego a more thorough characterization of the errors in our approximate spectrum computations until a more accurate code is available, but the approximations are likely accurate enough for reliable parameter analysis. It is unclear at this point whether the errors in our approximations or the systematic errors in CMBFAST will have a greater impact on the inferred error region. (Several other public CMB Boltzmann codes are in fact available, but none are as general as CMBFAST, allowing for arbitrary curvature, vacuum energy, and neutrino species, all of which are required for the analysis presented here.)

V. DISCUSSION AND CONCLUSIONS

Error regions similar to Fig. 9 have been previously constructed for model microwave background experiments [10, 38]. The remarkable point about our calculation is that the entire error region, constructed from power spectra for 3×10^4 points in parameter space, has been computed in a few seconds of time on a desktop computer. In fact, since our power spectra can be computed with a few arithmetic operations per multipole moment, the calculation time might not even be dominated

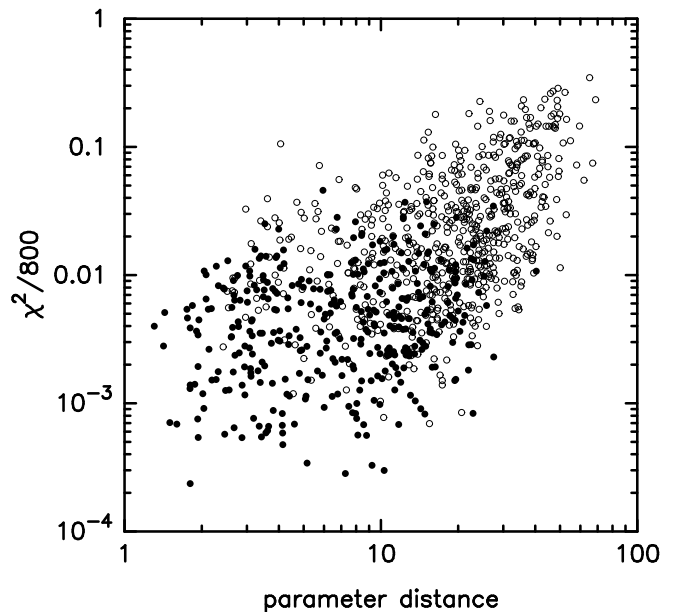


FIG. 11: A plot of the difference between approximate and numerical power spectra versus distance from the fiducial model in parameter space, for 1000 cosmological models drawn randomly from the distribution in Fig. 7. The solid circles are for models with $2 < N_\nu < 4$.

by computing model power spectra, but rather by computing the likelihood function or by converting between the cosmological and physical parameters.

For actual non-diagonal covariance matrices describing real experiments, the computation of the likelihood will dominate the total computation time. Gupta and Heavens have recently formulated a method for computing an approximate likelihood with great efficiency [40], based on finding uncorrelated linear combinations of the power spectrum estimates [41]. Each parameter corresponds to a unique combination, so the likelihood is calculated with a handful of operations. Moreover, the method is optimized so the parameter estimation can be done with virtually no loss of accuracy. Using this technique, likelihood estimates for realistic covariance matrices will be roughly as efficient as our power spectrum estimates.

The conversion from the physical parameters to cosmological ones requires evaluation of several numerical integrals. The integrands will be smooth functions, and this step can likely be made nearly as efficient as the power spectrum evaluation, although we have not implemented an optimized routine for parameter conversion. We make the following rough timing estimate: each multipole of the power spectrum can be approximated by a handful of floating point operations, and an approximate likelihood and the parameter conversion both will plausibly require similar computational work. So we anticipate on the order of 10 floating point operations per multipole for each of 1000 multipoles. On a 1 gigaflop machine, this results in evaluation of around 10^5 models per second, so a Markov Chain with tens of thousands of models can be

computed in under a second. Of course, such a computation is trivially parallelizable, and can easily be sped up by a factor of tens on a medium-size parallel machine. In contrast, other state-of-the-art parameter estimation techniques [16, 17, 23], dominated by the power spectrum calculation, compute roughly one model per second, requiring several hours for a 10^4 point computation.

This great increase in computational speed is highly useful. All upcoming microwave background measurements and resulting parameter estimates will be dominated by systematic errors, both from measurement errors when observing the sky and processing errors in the data analysis pipeline. The only way to discern the effect of these errors is through modelling them, requiring a determination of parameters numerous times. The microwave background has the potential to constrain parameters at the few percent level. But a variation of this size in any given parameter will result in changes in C_l 's of a few percent, which is significantly smaller than the errors with which each C_l will be measured. This means that small systematic effects distributed over many C_l 's can bias derived parameter values by amounts larger than the formal statistical errors on the parameter. Exhaustive simulation of a wide range of potential systematics will be required before the accuracy of highly precise parameter determinations can be believed, and our techniques make such investigations far faster and easier.

Along with increased speed, our approximation methods also promise high accuracy. A careful error evaluation is hindered by systematic errors in CMBFAST; our numerical approximations give better accuracy than the predominant numerical code for parameter ranges generally larger than the region which will be allowed by the MAP data. The physical set of variables presented here clarify the degeneracy structure of the power spectrum, clearly displaying degenerate and near-degenerate directions in the parameter space. For example, with the physical parameters presented here, it is clear that any tensor mode contribution, which affects only low- l multipoles, will have negligible impact on the error contours in Fig. 7.

Bond and Efstathiou used a principle component analysis to claim that uncertainties in the tensor mode contributions would be the dominant source of error for all of the cosmological parameters, and further claimed that as a result, the Fisher matrix approximation will overestimate the errors in other apparently well-determined parameters such as our \mathcal{B} [10]. These results are clearly valid only for data which is significantly less constraining than the MAP data will be. Essentially, their approximate degeneracy trades off variations in \mathcal{R} and \mathcal{B} , which change the heights of the first few peaks, with variations in n_s , which also impact the first few peaks, while holding \mathcal{A} fixed. From our analysis, it is clear that this degeneracy only holds approximately, since \mathcal{R} and \mathcal{B} have a significant impact only on the first three peaks, while n_s affects all of the peak heights. Indeed, a careful examination of Fig. 3 in [42] shows that the power spectra are

only approximately degenerate, with peak height differences which are significant for MAP. The addition of tensor modes allows a rough match between the two power spectra at low l values, but for high l values the discrepancy in peak heights is already evident at the third peak and will become larger for higher peaks, since the values of n_s in the two models are so different.

Gravitational lensing makes a negligible difference in the linearity of the parameter dependences. We have not included polarization in this analysis, but the three other polarized CMB power spectra can be handled in the same way as the temperature case using standard techniques [43, 44].

We have shown that a proper choice of physical parameters enables the microwave background power spectrum to be simply approximated with high accuracy over a significant region of parameter space. This region will be large enough for analyses of data from the MAP satellite, although larger regions could be stitched together using multiple reference models. Our approximation scheme requires first computing numerical derivatives of the power spectrum multipoles with respect to the various parameters, but this must be done only once and then computing further spectra is extremely fast (in the neighborhood of 10^5 models per second or more on common computers). The error determination techniques in this paper require the numerical evaluation of only tens of power spectra rather than thousands or millions, so speed of the power spectrum code will not be of paramount concern. On the other hand, we emphasize that for *any* high-precision parameter estimate, even small systematic errors in computing C_l 's can lead to biased parameter estimates comparable to the size of the statistical errors. These two considerations argue for a significant revision of CMBFAST (CMBSLOW, perhaps?) or construction of other independent codes which focus on overall accuracy and stability of derivatives with respect to parameters rather than on computational speed. Such a code, combined with the estimation techniques in this paper and efficient likelihood evaluation methods [40] will provide a highly efficient and reliable way to constrain the space of fundamental cosmological parameters.

Acknowledgments

We thank David Spergel, who has independently implemented some of the ideas in this paper, for helpful discussions, and Lloyd Knox, Manoj Kaplinghat, and Alan Heavens for useful comments. We also thank Uros Seljak and Matias Zaldarriaga for making public their CMBFAST code, which has proven invaluable for this and so much other cosmological analysis. A.K. has been supported in part by NASA through grant NAG5-10110, and is a Cotrell Scholar of the Research Corporation.

APPENDIX A: A MODEL PIPELINE FOR PARAMETERS ANALYSIS

In the interests of completeness, in this Appendix we outline an analysis pipeline for cosmological parameters and their errors. Our basic data set will be a high-resolution microwave background map, from which has been extracted an angular power spectrum (i.e., the C_l 's) and a covariance matrix for the C_l 's. Given this data set, plus potentially relevant data from other sources, we need to find the best-fit cosmological model and the error contours in the parameter space.

In the case of an ideal, full-sky map with only statistical errors and uniform sky coverage, the covariance matrix reduces to a multiple of the identity matrix, but in general, for most experiments the covariance matrix may contain significant off-diagonal terms. Even for the MAP satellite, which will come close to a diagonal covariance matrix, the need to mask out the galactic plane induces some correlations between nearby multipoles. The first step in the analysis is to construct a likelihood calculator: what is the likelihood that the measured data represents some particular theoretical power spectrum? This is in general a computationally hard problem, since it involves inverting an $N \times N$ matrix, where N is the number of multipoles in the power spectrum. However, the problem becomes easier if the covariance matrix is close to diagonal. Heavens and Gupta have recently formulated a method for computing an approximate likelihood with great efficiency [40], based on an eigenvector decomposition of the covariance matrix [41]. They have demonstrated a likelihood calculator which takes an input theoretical power spectrum and outputs a likelihood based on simulated measurements and covariances in much less than a second of computation time. Further efficiency improvements are desirable, as this is likely to be the piece of the analysis pipeline which dominates the total time.

The likelihood calculator can also incorporate prior probabilities obtained from other data sources, or from physical considerations like $\Lambda > 0$. Since none of the following steps depend on the form of the likelihood function, the inclusion of other kinds of data can be handled in a completely modular way.

The second element needed is a pair of routines to convert between the physical parameter space (\mathcal{A} , \mathcal{B} , \mathcal{M} , \mathcal{V}) and the cosmological parameter space (Ω_{mat} , Ω_b , Ω_Λ , h). To go from the cosmological parameters to the physical parameters simply involves evaluating the integral needed in Eq. 8. The reverse direction can be done straightforwardly by rewriting \mathcal{A} in terms of \mathcal{B} , \mathcal{M} , \mathcal{V} , \mathcal{R} , and h and then numerically finding the value of h which gives the needed value of \mathcal{A} . The total variation of \mathcal{A} with h is a smooth function, and the root-finding step can be done with a minimal number of integral evaluations. This procedure does not guarantee a solution, however, in extreme regions of parameter space. A more general (but slower) method is to search the cosmolog-

ical parameter space for the model which best fits the given set of physical parameters, and then project this model back into the physical parameter space to check the quality of the fit.

Once a likelihood calculator and parameter conversion routines are in hand, we advocate the following procedure for parameter determination. First, choose a fiducial model which gives a good fit to the measured power spectrum. This can largely be done by eye, using the parameter dependences displayed in the Figures in Sec. III. Note that the fiducial model does not need to be the formal best-fit model, but only needs to be close enough to the best-fit model so that models throughout the error region will be accurately approximated by the extrapolations and approximations in Sec. III.

Next, check the validity of the fiducial model. Is the fit of the model with the data adequate? It is certainly possible that the simple space of cosmological models considered here may not contain the actual universe. For example, some admixture of isocurvature initial conditions might be important, or the initial power spectrum might not be well described by a power law. If the best-fit model is not a good fit to the data, it makes no sense to proceed with any further parameter analysis! The model space must be enlarged or modified to include models which provide a good fit to the data.

If the fiducial model is adequate, then compute numerical partial derivatives of each C_l with respect to \mathcal{B} , \mathcal{M} , and \mathcal{R} . Also, write numerical routines to compute the power spectrum approximately for $l < 50$. Even though CMBFAST or similar codes run very efficiently when computing only $2 < l < 50$, this time will still greatly dominate the total computation time for parameter error determination, so an efficient analytic estimate is essential. Note that an alternate possibility is to simply ignore the lowest multipoles, which will be a small portion of the data for a high-resolution map, at the expense of losing any leverage on the parameters \mathcal{V} , \mathcal{Z} , and the tensor power spectrum. Still, the other parameters will be determined much more precisely, so it may be possible to fit the rest of the parameters using $l > 50$ data only, and then constrain just the \mathcal{V} - \mathcal{Z} -tensor parameter space from the $l < 50$ data independently. Now it is possible to estimate the C_l 's highly efficiently for any model within a sizeable parameter space region around the fiducial model.

Now perform a Markov-chain Monte Carlo [15] in the physical parameter space. Each point in parameter space requires evaluation of one approximate power spectrum, one likelihood, and one conversion to cosmological parameters. The Monte Carlo will converge efficiently since the physical parameters are nearly orthogonal in their effects on the power spectrum. Sophisticated convergence diagnostics are available for determining when the Markov chain of models has sufficiently sampled the error region [45].

Finally, once the chain of models in parameter space has been computed, extract the best-fit model and error

contours from the distribution of models. By displaying two-dimensional likelihood plots for all parameter combinations, a reliable picture of the shape of the likelihood region in the whole multidimensional parameter space can be visualized.

Upcoming data will be good enough that the statistical errors, given by these likelihood contours, will be smaller than the systematic errors, at least in some parameter space directions. Sources of systematic error include instrumental effects, modelling of foreground emission, approximation of the covariance matrix, inaccuracies in the theoretical models, and inaccuracies in the approximations in this paper. Before we can confidently claim to have determined the cosmological parameters and their errors, these systematics must be modelled and investigated. Using the techniques outlined here, where a complete Monte Carlo can be accomplished in seconds, investigation of systematics is easily practical, instead of a computational challenge.

APPENDIX B: SOME NUMERICAL CONSIDERATIONS WITH THE CMBFAST CODE

Seljak and Zaldarriaga’s CMBFAST code [33, 35] has become the standard tool for computing the microwave background temperature and polarization power spectra for the inflation-type cosmological models discussed in this paper. Hundreds of researchers have employed it for tasks ranging from predictions of highly speculative cosmological models to analysis of every microwave background measurement of the past few years. Its comprehensive treatment of a variety of physical effects and its public availability have made it the gold standard for microwave background analysis.

The original aim of the CMBFAST code was fast evaluation of the power spectra. Previous codes had simply evolved the complete Boltzmann hierarchy of equations up to the maximum desired value of l . This resulted in a coupled set of around $3l$ linear differential equations, and the l -values of interest might be 1000 or greater. The task of evolving thousands of coupled equations with oscillatory solutions led to codes which required many hours to run on fast computers. The CMBFAST algorithm evolves the source terms first, which involve angular moments only up to $l = 4$; the same Boltzmann hierarchy can be used, but with a cutoff of $l \simeq 10$. The rest of the C_l ’s can then be obtained by integrating this source term against various Bessel functions. The Bessel functions can be precomputed or approximated [46] independently for each l . Great time savings result since (1) it is not necessary to compute the power spectrum for every l , but rather only, e.g., every 50th l with the rest obtained from interpolation; (2) the time steps for the Boltzmann integration are not controlled by the need to resolve all of the oscillations in the Bessel functions, and thus the Boltzmann integrator can be significantly more efficient.

It also may be possible to employ approximations to the integrals of the source times the Bessel functions with an additional gain in speed, although CMBFAST does not implement this. The code offers a speed improvement of a factor of 50 over Boltzmann hierarchy codes for flat universes, although the advantage is smaller for models which are not flat or have a cosmological constant.

CMBFAST is nominally accurate at around the one percent level, although no systematic error analysis has ever been published. While the numerical error in any given multipole C_l is relatively small, the derivatives of C_l with respect to the various cosmological parameters are significantly less accurate. At the time the code was written, no microwave background experiments were of sufficient precision to warrant worrying about inaccuracies at this level, and the great utility of the code has been its combination of speed and accuracy. But we have now entered the era of high-precision measurements which will place significant constraints on many parameters simultaneously, and as this paper has demonstrated, efficiently prosecuting this analysis requires a code of high precision and stable behavior with respect to parameter variations. We have found that the unmodified version of CMBFAST “out of the box” is not sufficiently accurate for the calculations presented here, but these shortcomings are partially compensated by the following procedures.

First, CMBFAST uses slightly different algorithms for flat and non-flat background spacetime geometries. In the flat case, the necessary spherical Bessel functions are precomputed and called from a file; in the nonflat case, the hyperspherical Bessel functions are computed via an integral representation as they are needed. As a result, the line-of-sight integrals over the product of source term and Bessel function have different partitions in the two cases, and the numerical values differ at the percent level. Also, the code has a flag which forces evaluation of the flat case whenever $|\Omega - 1| < 0.001$. If the fiducial model is flat, then as parameters are varied which change the geometry, many individual multipoles C_l exhibit discontinuities at the point in parameter space where the code switches from the flat to nonflat evaluation scheme. These discontinuities can result in significant errors when evaluating C_l derivatives with respect to parameters. Also, even if the derivative is correctly evaluated, the offset between the two cases can result in a slightly biased error estimate.

A careful fix of this problem would involve insuring that the integral partitions used in the two cases are determined consistently. Alternately, the flat-space code could be rewritten to numerically integrate the necessary Bessel functions as in the non-flat case, since the two methods do not have a significant difference in computational speed. A simpler practical solution which we have employed in this paper is to force the code always to use the non-flat integration routine. This can be accomplished by narrowing the tolerance at which the code uses the non-flat integration (say to $|\Omega - 1| < 10^{-5}$), combined with always using a non-flat fiducial model (shifting Ω_{mat}

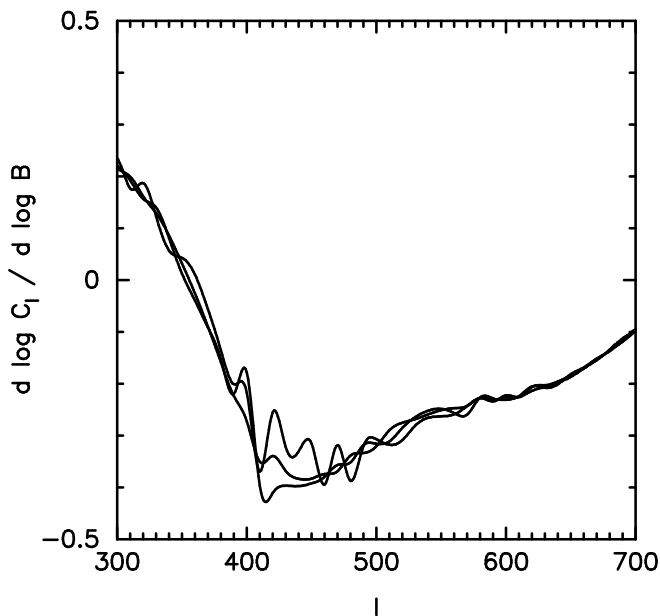


FIG. 12: Derivatives of C_l with respect to \mathcal{B} , calculated by CMBFAST with $\Delta l = 10$, from 2%, 5%, and 10% finite differences in \mathcal{B} . The smoothest curve is for the 10% variation.

by 10^{-5} will never result in a statistically significant difference when fitting a given data set, due to cosmic variance).

Second, in varying the \mathcal{B} parameter, adjacent acoustic peaks move in the opposite direction. Between the peaks, therefore, is a pivot point l for which C_l remains fixed as \mathcal{B} is varied, and the nearby C_l 's will vary only slightly. As CMBFAST is written, it computes C_l at l values separated by 50; the complete spectrum is then obtained by splining between the calculated values. Splines are rather stiff, and small changes in regions where the power spectrum has significant curvature (i.e. around the acoustic peaks and troughs) can noticeably change the overall fit to the power spectrum in the regions between. In particular, the position of the ‘‘pivot’’ l -value in the spectrum sometimes shifts a bit, which gives a spurious irregular dependence on \mathcal{B} of the few C_l 's in this region.

This can be addressed by a simple modification to CMBFAST forcing the explicit evaluation of C_l for more l values. We have used a δl of 10, which has eliminated

the spurious behavior. Of course, this results in a significant increase in the computational time needed for an individual model. A more sophisticated approach would be to use a comparable number of l values as the original code, but distribute them preferentially in the l -ranges corresponding to the peaks and troughs where the curvature of the power spectrum is largest. This is easily implemented using the variables defined in this paper, since the peak positions are completely determined by \mathcal{A} alone. Using a finer grid in l also reproduces the peak positions with higher accuracy.

Third, as discussed in the body of the paper, the power spectra must be normalized according to a physical criterion which does not depend on non-linear behavior at small l values. This is accomplished by simply compiling CMBFAST with the UNNORM option. In this case, no normalization to COBE is done; instead, the amplitude of the potential Ψ is taken to be unity at the scale of the horizon at the time of last scattering. This normalization is fixed by the primordial amplitude of scalar perturbations, often denoted as A_S . We define a physical variable S corresponding to the microwave background amplitude by also including the effect of differing amounts of reionization so that the power spectrum at large l remains fixed.

Some residual numerical problems remain with CMBFAST. We have found, for example, that in the region around $l = 350$ (between the first and second acoustic peaks for our fiducial model), the power spectrum exhibits spurious oscillatory behavior with an amplitude of a few percent, if computed directly for every l instead of every 10th or 50th l (see Fig. 12). This likely arises from either the k or η integral over an oscillatory integrand not being evaluated on a fine enough grid. As a result, directly calculated C_l values in this region of the parameter space effectively have non-negligible random errors. This problem is normally hidden by the spline smoothing with every 50th l computed. When the number of C_l evaluations is increased to every 10th l , the power spectrum shows a distinct glitch in this region, and the parameter dependence is completely unreliable here. The spline fits are forced into more oscillations to include the computed points. More accurate numerical integrations will probably solve this problem, at the expense of a significant speed reduction.

[1] URL <http://map.gsfc.nasa.gov>.

[2] P. de Bernardis, P. A. R. Ade, J. J. Bock, J. R. Bond, J. Borrill, A. Boscaleri, K. Coble, B. P. Crill, G. De Gasperis, P. C. Farese, et al., *Nature (London)* **404**, 955 (2000).

[3] S. Hanany, P. Ade, A. Balbi, J. Bock, J. Borrill, A. Boscaleri, P. de Bernardis, P. G. Ferreira, V. V. Hristov, A. H. Jaffe, et al., *Astrophys. J.* **545**, L5 (2000).

[4] N. W. Halverson, E. M. Leitch, C. Pryke, J. Kovac, J. E. Carlstrom, W. L. Holzapfel, M. Dragovan, J. K.

Cartwright, B. S. Mason, S. Padin, et al., *Astrophys. J.* **568**, 38 (2002).

[5] M. Kamionkowski and A. Kosowsky, *Ann. Rev. Nuc. Part. Sci.* **49**, 77 (1999).

[6] W. Hu and S. Dodelson, *Ann. Rev. Astron. Astrophys.* **in press** (2002).

[7] A. Kosowsky, in *Modern Cosmology*, edited by S. Bonometto, V. Gorini, and U. Moschella (IOP Publishing, Bristol and Philadelphia, 2002), p. 219.

[8] G. Jungman, M. Kamionkowski, A. Kosowsky, and

- D. Spergel, Phys. Rev. D **54**, 1332 (1996).
- [9] J. R. Bond, R. Crittenden, R. L. Davis, G. Efstathiou, and P. J. Steinhardt, Phys. Rev. Lett. **72**, 13 (1994).
- [10] J. Bond and G. Efstathiou, Mon. Not. R. Ast. Soc. **304**, 75 (1999).
- [11] K. M. Gorski, G. Hinshaw, A. J. Banday, C. L. Bennett, E. L. Wright, A. Kogut, G. F. Smoot, and P. Lubin, Astrophys. J. **430**, L89 (1994).
- [12] M. Tegmark and M. Zaldarriaga, Astrophys. J. **544**, 30 (2000).
- [13] S. Dodelson and L. Knox, Phys. Rev. Lett. **84**, 3523 (2000).
- [14] A. Melchiorri, P. A. R. Ade, P. de Bernardis, J. J. Bock, J. Borrill, A. Boscaleri, B. P. Crill, G. De Troia, P. Farese, P. G. Ferreira, et al., Astrophys. J. **536**, L63 (2000).
- [15] N. Christensen, R. Meyer, L. Knox, , and B. Luey, Class. Quant. Grav. **18**, 2677 (2001).
- [16] D. Spergel, private communication (2002).
- [17] L. Knox, N. Christensen, and C. Skordis, Astrophys. J. Lett. **563**, 95 (2001).
- [18] S. Dodelson and A. Kosowsky, Phys. Rev. Lett. **75**, 604 (1995).
- [19] M. Zaldarriaga, D. Spergel, and U. Seljak, Astrophys. J. **488**, 1 (1997).
- [20] J. Bond, G. Efstathiou, and M. Tegmark, Mon. Not. R. Ast. Soc. **291**, L33 (1997).
- [21] D. J. Eisenstein, W. Hu, and M. Tegmark, Astrophys. J. **518**, 2 (1999).
- [22] L. Griffiths and A. Melchiorri, New Astron. Rev. **45**, 321 (2001).
- [23] M. Kaplinghat, L. Knox, and C. Skordis (2002), astro-ph/0203413.
- [24] W. Hu and N. Sugiyama, Astrophys. J. **444**, 489 (1995).
- [25] W. Hu and N. Sugiyama, Phys. Rev. D **51**, 2599 (1995).
- [26] W. Hu and N. Sugiyama, Astrophys. J. **471**, 542 (1996).
- [27] W. Hu and M. White, Astrophys. J. **471**, 30 (1996).
- [28] S. Weinberg, Phys. Rev. D **64**, 123511 (2001).
- [29] S. Weinberg, Phys. Rev. D **64**, 123512 (2001).
- [30] J. Peacock, *Cosmological Physics* (Cambridge Univ. Press, 1999).
- [31] E. Bunn and M. White, Astrophys. J. **480**, 6 (1997).
- [32] A. Kosowsky and M. Turner, Phys. Rev. D **52**, R1739 (1995).
- [33] U. Seljak and M. Zaldarriaga, Astrophys. J. **469**, 437 (1996).
- [34] M. Zaldarriaga, U. Seljak, and E. Bertschinger, Astrophys. J. **494**, 491 (1998).
- [35] M. Zaldarriaga and U. Seljak, Astrophys. J. Suppl. **129**, 431 (2000).
- [36] M. Zaldarriaga, Phys. Rev. D **55**, 1822 (1997).
- [37] R. Durrer, B. Novosyadlyj, and S. Apunevych (2001), astro-ph/0111594.
- [38] A. Lewis and S. Bridle (2002), astro-ph/0205436.
- [39] L. Knox, Phys. Rev. D **52**, 4307 (1995).
- [40] S. Gupta and A. Heavens (2001), astro-ph/0108315.
- [41] A. F. Heavens, R. Jimenez, and O. Lahav, Mon. Not. R. Ast. Soc. **317**, 965 (2000).
- [42] G. Efstathiou, Mon. Not. R. Ast. Soc. **332**, 193 (2002).
- [43] M. Kamionkowski, A. Kosowsky, and A. Stebbins, Phys. Rev. D **55**, 7368 (1997).
- [44] M. Zaldarriaga and U. Seljak, Phys. Rev. D **55**, 1830 (1997).
- [45] W. Gilks, S. Richardson, and D. Spiegelhalter, *Markov Chain Monte Carlo in Practice* (Chapman and Hall, 1996).
- [46] A. Kosowsky (1998), astro-ph/9805173.